Variable Topology "Tree-Like" Continuum Robots for Remote Inspection and Cleaning

Michael C. Lastinger
Department of Electrical and Computer Engineering
Clemson University
Clemson, SC 29634
mlastin@clemson.edu

Allyanna Rice
Department of Electrical and Computer Engineering
Clemson University
Clemson, SC 29634
allyanr@clemson.edu

Apoorva Kapadia
Department of Electrical and Computer Engineering
Clemson University
Clemson, SC 29634
akapadi@clemson.edu

Ian D. Walker
Department of Electrical and Computer Engineering
Clemson University
Clemson, SC 29634
iwalker@clemson.edu

***Abstract*—We discuss a novel variable topology continuum robot designed and constructed under NASA-funded research. The robot features a seven degree of freedom continuous backbone "trunk", with two pairs of "branches": two "tendril" effectors and two support "roots". Each of the pairs of branches can be fully retracted inside the trunk, allowing it to penetrate congested environments as a single slender unit, and subsequently deploy the branches to perform a variety of tasks. The "roots" provide physical support, while the two effectors and trunk tip enable independent but coordinated functionality: sensing (vision) in one tendril, and manipulation at two scales, via the second tendril and the trunk tip. The specifics of the new design are described and discussed in detail. We illustrate the operation and potential applications of the new design via a series of demonstrations, particularly cleaning of dust from solar panels.**

TABLE OF CONTENTS

1. INTRODUCTION

Conventional robot manipulators are heavy, and poor in accessing congested spaces due to the constraints imposed by their rigid links. Their use often relies on the additional deployment of sensor heads, which can be bulky, and also difficult to deploy in tight spaces.

978-1-7821-2734-7/20/$31.00 ©2020 IEEE

In this paper, we introduce a novel, light, continuously bending "tree-like" robot with retractable branches (Figure 1). We demonstrate its ability for unique and adaptive operations over multiple scales and discuss the potential for use of such robots in operations in Space.

Figure 1. Variable topology continuum TREE robot

The robot design considered herein features compliant continuous backbone elements, and is thus an example of a continuum robot [16],[19]. The sub-field of robotics focusing on continuum "trunk and tentacle" robots has seen a surge of

interest and activity in recent years, enabling a number of new and innovative applications [1],[4], particularly in medical procedures [2].

Continuum robots have been proposed for Space applications previously. NASA developed the first long, thin "tendril" continuum robot [9], with the aim of penetrating and interrogating congested spaces infeasible with conventional rigid-link-based robotic structures. More recent efforts have refined the tendril design [15],[18], aiming at inspection operations on the International Space Station [20],[21].

The key innovation in the robot design discussed here is in its parallel and variable topology structure. Two pairs of independently controlled "branches" can be extended from the central "trunk" (hence the acronym TREE, from Tree Robot for Extended Environments). This provides the capability to configure from a single trunk (with the branches fully retracted) to a wide variety of parallel topologies. This allows the robot to enter and maneuver within tight spaces, and then configure to present multiple sensor views and/or manipulators to its environment.

The advantages of such parallel robotic structures in Space environments has been demonstrated previously, notably in the multi (rigid-link)-limbed Dextre robot [3]. However, the use of parallel continuum structures is new, and can provide novel functionality, as discussed in this paper.

The design concept and prototype realization of the proposed robot is presented in Section 2 of this paper. Section 3 describes validation experiments with the prototype, and Section 4 discusses representative experiments, focused towards solar panel cleaning. Section 5 provides a summary of the paper.

2. ROBOT DESIGN AND PROTOTYPE

The TREE design, introduced in [7], features a core trunk with emerging continuum branches. In [7], a hardware prototype of the design and initial testing with it were described. In this section we review the prototype and its functionality. We then present for the first time a kinematic model of the trunk. Results from a series of experiments evaluating the capabilities and operational potential of the design are reported in subsequent sections of the paper.

All elements (trunk and branches) of the robot are continuum structures. Continuum robots possess significant advantages compared to traditional rigid-link robot structures: they are simple, lightweight, compliant, and relatively inexpensive [17]. This makes continuum robots an attractive option for deployment in Space environments and operations.

Trunk

The trunk of the TREE robot is formed from three concentric tubes, composed of plastic composite material. Each tube can be bent via remote actuation of two tendons, spaced 180 degrees apart radially, which are routed via periodic spacers along the outside of the tubes. Bending occurs in the plane in which the pair of tendons lie. Each of the two distal tubes retract into the immediately preceding one, with extension and retraction driven by linear actuators at the base of the structure. The two more distal tubes are free to rotate within the preceding tubes, with this rotation also actuated remotely at the base.

In total, this design provides the trunk with seven degrees of freedom (3 in bending, and two each in extension/retraction and rotation). Kinematically, this results in three "sections" (tubes), with one (bending), three (extension/retraction, bending, and rotation of plane of bending), and three (extension/retraction, bending, and rotation of plane of bending) degrees of freedom, from base to tip, respectively. See [7] and Figure 1.

The interior of the trunk is largely hollow. This provides space for the housing of the two pairs of "branches". These branches, when retracted into the trunk, are housed within tubes in its interior. Outlets to these tubes are created at fixed locations in the trunk surface to allow ingress and egress of the branches.

Branches

The four (two pairs of) branches are independently actuated to extend and retract from the trunk. The more distal pair, termed "tendrils", are of a tendon-actuated design, featuring thin concentric carbon fiber tubes. Multi-section versions of this design have been extensively investigated by our group previously [20] in the context of investigating single tendril inspection operations on the International Space Station [21]. In the TREE prototype, the implemented tendrils each have two sections, each with two degrees of freedom (remotely actuated bending in two dimensions), resulting in five degree of freedom branches when including extension/retraction from the trunk. See [7] and Figure 1. The main function of the tendrils is to remotely locate sensors and end effectors in coordination with the tip of the trunk. This can provide novel functionality, as will be demonstrated in the following sections.

The more proximal (in terms of the location of its emergence from the trunk, with respect to the base) pair are termed herein "roots". The core structural elements of the roots are interlocking "vertebrae" connected by a central spring. When the spring is uncontracted, these vertebrae are unconnected, and remotely actuated tendons routed through them bend the branches into desired shapes. Given a desired shape, the spring can be remotely contracted with a single linear actuator to lock the vertebrae and stiffen these "root" branches. This provides the main functionality of the roots: as support (stiffening) elements for the more distal branch/tendril elements. Such stiffening is highly beneficial in compliant continuum structures, as it decouples wrenches at the tip from the part of the robot proximal to the stiffening elements [20].

Control System

The TREE trunk was controlled using closed-loop position feedback (to the Rhino DC Servo motors actuating it). When controlling the trunk, the Rhino motors were commanded at the level of encoder counts (motor positions) sent to the motors.

An Arduino Mega was used to control the trunk. The Mega had about 4 KB of EEPROM storage on-board which was sufficient for our purposes. Arduino has an open-source EEPROM library that made interfacing with the memory a matter of executing "read," "write," or "update" commands. The encoders of the Rhino motors read 1800 counts per revolution. Due to the construction of the TREE trunk (materials), the assumption that no motor should ever need to travel greater than one revolution was a safe one. Therefore, assuming a maximum possible encoder count of 1800 that may need to be stored, we elected to scale the encoder positions down by a factor of 15 before saving them to EEPROM.

The TREE branches were controlled using an Arduino Due. To ensure the functionality of the robot was that of one cohesive system (trunk and branches), the Due was set up to communicate serially with the Mega. The Mega was established as the master device and the Due as the slave. The results enabled effective closed-loop control of the TREE.

Kinematics

A kinematic model was developed for and implemented on the trunk. Forward kinematics takes encoder counts and tendon lengths in the actuator space and converts them into the configuration (shape) of the robot via a suitable homogeneous transformation matrix. The approach to formulating the forward kinematics model implemented on the TREE is based on the model described in [5]. This approach uses a modified version of the Denavit-Hartenberg convention (commonly used to implement forward kinematics model for rigid-link robots), to develop the kinematics of constant curvature continuum robots. The shape parameters used in the model for each section are its arc length s, curvature k, and rotation out of the plane φ.

The shapes of the sections of the TREE assume approximately constant curvature, so the above approach was determined to be suitable for its modeling. For the TREE, because it is a multi-section robot with the configuration of each section defined by a separate (s, k, φ), a homogeneous transformation matrix was formed for each of the sections. The final transformation matrix describing the shape/configuration of the entire trunk is the result of those three section matrices multiplied together.

For the TREE sections, s is straightforward to calculate as simply its physical length. The length of the middle section is measured from the point it emerges from the proximal section tube. This is sensed via the addition of ultrasonic distance sensors which keep track of how much (and in which direction) the middle section moves. A similar procedure is used to sense the distal section arc length of the TREE. Note that one important consideration is that as the middle section changes length, the effective length of the distal section changes regardless of whether or not is has been actuated. Therefore, it is not sufficient to merely determine the length of the tip section based on the reading from the distance sensor.

The curvature, k, of each section for this tendon arrangement is derived in [5] as

$$k = \frac{(l_1 - l_2)}{d(l_1 + l_2)} \tag{1}$$

where l_1 and l_2 are the lengths of the tendons, measured in cm, and d is the (fixed) radius of the section (tube) in cm. The above expression assumes constant curvature of the section, implying that the shape of the section can be modeled by the curvature (the inverse of the radius of the circular segment traced in space by the section). In order to calculate this curvature for the TREE, it was necessary to relate changes in encoder counts to changes in tendon lengths. We initially considered trying to predict this change by using the inner radius (to determine circumference) of the tendon spools to calculate the changes in length based on motor rotation. This proved impractical due to the non-uniform way in which the tendons wind onto the spools. Performing the calculations under the assumption that the winding is uniform produces inaccurate results. Therefore, we empirically estimated the encoder count/tendon length relationship. The measured data, shown in Figure 2, reveals that this relationship is nonlinear. We therefore generated a best fit quadratic, shown as the dotted line in Figure 2, to approximate a function that represents the data.

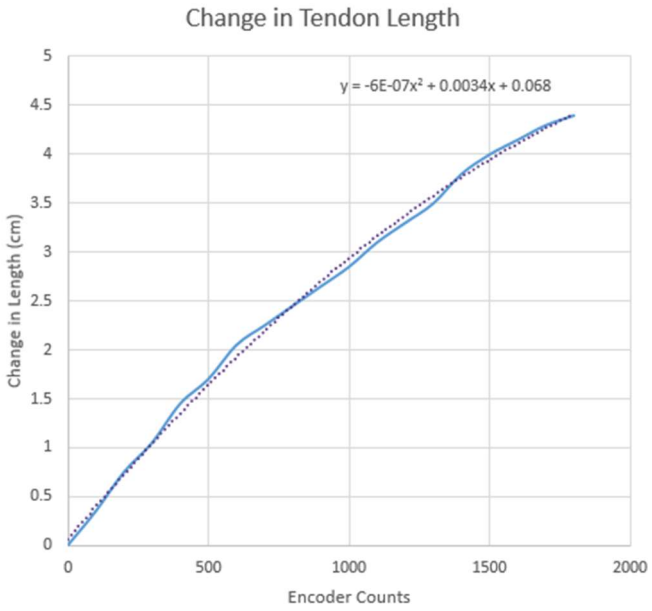

Figure 2. Experimental data relating encoder counts to tendon lengths

The equation for the best fit quadratic was found empirically to be

$$y = -(6E-07)x^2 + 0.0034x + 0.068 \quad (2)$$

where x is encoder counts and y is the corresponding change in length, Δl.

The shape parameter φ is also straightforward to determine for each of the sections of the TREE. This angle of rotation, in the x-y (left-right) plane (see Figure 4) at the base of each section can be directly determined using the current encoder counts of the rotational motors for the middle and distal sections. (The proximal section cannot rotate.) Given the middle section gear reduction ratio of

$$\frac{45}{11} = 4.09:1 \quad (3)$$

and with the motor encoder having 1800 counts per revolution (CPR), the total number of encoder/motor counts required for 1 revolution of the middle section is

$$4.09 * 1800 \text{ counts} = 7362 \text{ counts} \quad (4)$$

Similarly, given the distal section gear reduction ratio of

$$\frac{24}{11} = 2.18:1 \quad (5)$$

and this motor's encoder also having 1800 CPR, the total number of counts required for 1 revolution of the distal section is

$$2.18 * 1800 \text{ counts} = 3924 \text{ counts} \quad (6)$$

Finally, φ (positive for counterclockwise rotation) is expressed in radians, for each section.

Since the base section cannot rotate, we can use the planar model developed in [17], based on the transformation shown in Figure 3, to best approximate the kinematics for this section. This planar concept approximates the kinematics of a continuum robot based on that of a virtual planar RPR (revolute-prismatic-revolute joint) rigid-link robot, formulating the kinematics in terms of its (virtual) variables, and then converting to the continuum variables). Using this model and the shape parameters defined above (note that φ is constant and set to zero in this planar case), the homogeneous transformation matrix of the proximal section of the TREE is given by:

$$[\mathrm{H}_3^0]_{\text{proximal}} = \begin{bmatrix} \cos(sk) & -\sin(sk) & 0 & \frac{1}{k}(\cos(sk)-1) \\ \sin(sk) & \cos(sk) & 0 & \frac{1}{k}\sin(sk) \\ 0 & 0 & 1 & 0 \\ 0 & 0 & 0 & 1 \end{bmatrix} \quad (7)$$

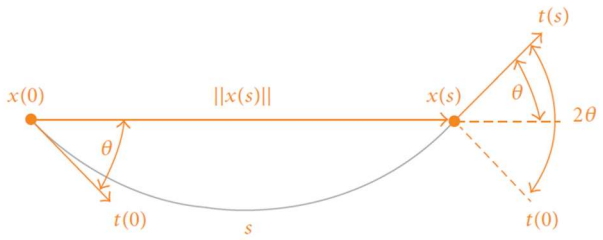

Figure 3. Planar concept used for modeling [17]

The middle and distal sections can rotate out of the x-y plane, so we elected to use the spatial model developed in [17], based on the coordinates and transformation shown in Figure 4 to best approximate the kinematics for these sections. The spatial model approximates the kinematics of a continuum robot based on that of a virtual spatial RRPR (revolute-revolute-prismatic-revolute joint) rigid-link robot. Using this model and the s, k, φ shape parameters defined above, the homogeneous transformation matrices of the middle and distal (tip) sections are

$$[\mathrm{H}_4^0]_{\text{middle}} = [\mathrm{H}_4^0]_{\text{distal}} =$$

$$\begin{bmatrix} \cos(\varphi)\cos(sk) & -\sin(\varphi) & -\cos(\varphi)\sin(sk) & \frac{1}{k}(\cos(\varphi)-\cos(\varphi)\cos(sk)) \\ \sin(\varphi)\cos(sk) & \cos(\varphi) & -\sin(\varphi)\sin(sk) & \frac{-1}{k}(\sin(\varphi)-\sin(\varphi)\cos(sk)) \\ \sin(sk) & 0 & \cos(sk) & \frac{1}{k}\sin(sk) \\ 0 & 0 & 0 & 1 \end{bmatrix} \quad (8)$$

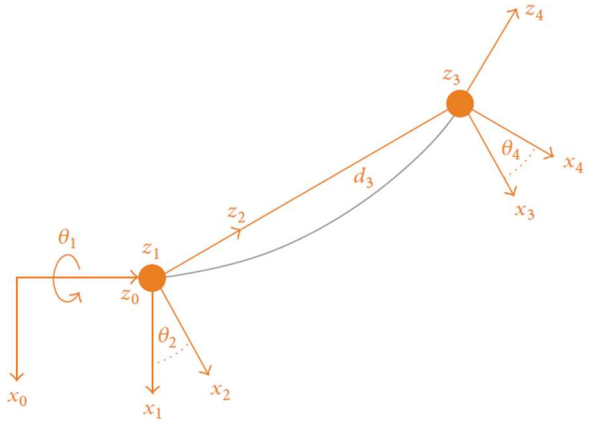

Figure 4. Spatial concept for modeling an RRPR rigid-link robot [17]

The upper left 3x3 matrix of equations (7) and (8) is the rotation matrix describing the shape/configuration of that particular section of the trunk, with respect to a local coordinate frame fixed in its base. The upper right 3x1 matrix is the translation vector, which describes the x, y, z coordinates of the end effector (i.e. the end of that section) with respect to a local coordinate frame fixed in its base. To

calculate the overall homogeneous transformation of the entire TREE trunk, the matrix given in equation (7) is multiplied by two matrices of the form in equation (8) as mentioned previously. The resulting transformation matrix for the TREE is

$$[H]_{\text{TREE}} = [H_3^0]_{\text{proximal}} * [H_4^0]_{\text{middle}} * [H_4^0]_{\text{distal}} \quad (9)$$

As with the section matrices, the upper left 3x3 matrix of equation (9) is the overall rotation matrix describing the shape/configuration of the entire TREE trunk. The upper right 3x1 matrix is the overall translation vector, which describes the *x*, *y*, *z* coordinates of the end effector (i.e. the tip of the TREE) with respect to the fixed base coordinate frame. Validation experiments of the kinematic model were conducted on top of a 10 cm x 10 cm grid as shown in Figure 5, with the model shown to be effective in modeling the kinematics.

Figure 5. TREE trunk prototype [7] on 10 cm x 10 cm grid (top view)

3. PROTOTYPE VALIDATION

Trunk Adaptability

An advantage of the extensible trunk with the branches retracted is that it can reach into areas which are difficult to access. To demonstrate this, we extended the robot into a long pipe which required it to bend about 90 degrees to inspect the distal part of the pipe. The tube extends approximately two feet into the pipe and then bends to the right (Figure 6).

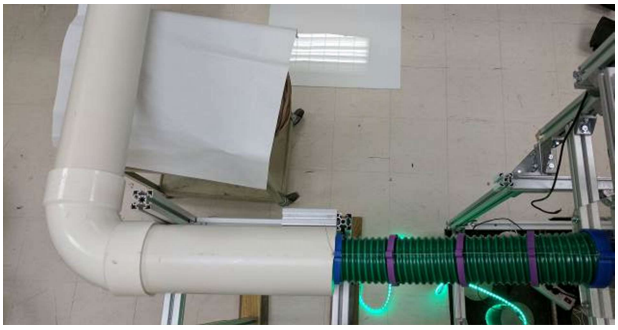

Figure 6. A 1.8 feet straight section of the pipe followed by a 90-degree bend

Inside the tube, a toy pumpkin which had illuminated eyes was placed (Figure 7).

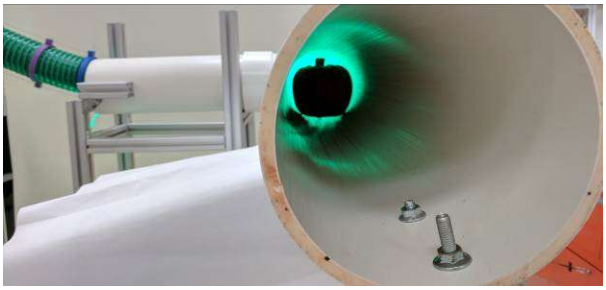

Figure 7. Pumpkin inside the tube illuminated by an LED strip

The entire robot assembly was mounted on a mobile base which can be moved on flat surfaces in order to orient the robot as required. The distal section had a camera attached to its end enabling teleoperation of the robot inside the pipe. The first step was to move the base towards to pipe in order to get the sections appropriately oriented to the entrance of the pipe. The proximal section was actuated in order to align the middle section with the tube entrance.

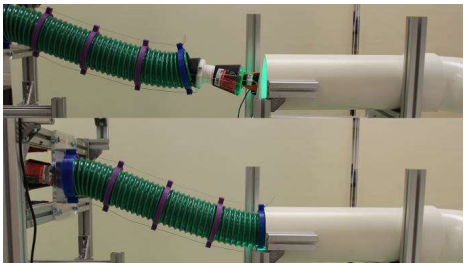

Figure 8. Alignment of the sections

Once the tip of the middle and the distal section were properly aligned, we extended the middle and distal sections inside the tube simultaneously (Figure 8). This was done by observing the movement of the sections through the camera mounted on the tip of the distal section. Once the section had reached the appropriate depth, the distal section was bent and after the tip section worked its way around the bend, the pumpkin inside the tube could be clearly seen (Figure 9). This experiment demonstrates the maneuverability of the core trunk of the TREE.

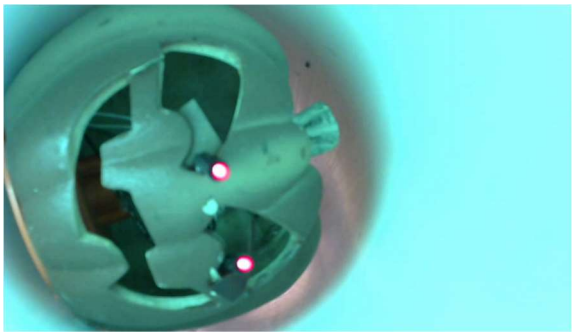

Figure 9. Image of pumpkin from camera on the distal section

4. REPRESENTATIVE EXPERIMENTS

Potential Applications

In this section, we discuss novel potential applications for the TREE. We empirically simulated several of these potential applications with the TREE in which the unique advantages of such a novel type of robot is demonstrated. The robot was required to perform representative tasks exploiting its branches, taking advantage of its variable topology and the ability to adapt to different environments.

Solar Panel Cleaning

There are a wide range of potential application fields for this novel design of a branching, concentric tube continuum robot. For example, consider applications where the trunk is blowing air/dusting and the two Tendril branches are assisting through inspection and delicate manipulation. One field that could find such robots useful is the aerospace industry (notably NASA). NASA relies on solar panels to power satellites, rovers, and other equipment while in space. In locations such as Mars, various atmospheric events like wind, storms, etc. can cause dust to build up on the solar panels hindering their ability to collect energy as detailed in [6].

Figure 10 shows an example of such dust accumulation on NASA's Mars Exploration Rover, Spirit. The left image in Figure 10 is a panoramic self-portrait of Spirit taken on August 27, 2005 [11]. It shows the solar panels with only a thin layer of dust two years after the rover landed and began exploring Mars. The right image of Spirit was assembled from frames taken between October 26-29, 2007 [12]. It shows the significant amount of dust that had accumulated on the solar panels of the rover, which reduced its ability to collect energy from the Sun.

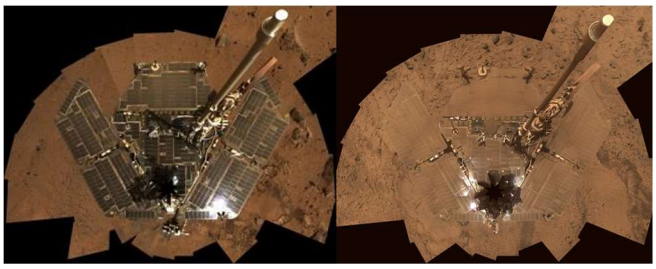

Figure 10. NASA's Mars Exploration Rover, Spirit, before (left [11]) and after (right [12]) dust accumulated on Solar Panels. Images courtesy of NASA/JPL-Caltech/Cornell University

Sometimes, the same windstorms that deposit dust on the rovers' solar panels fortuitously blow the accumulated dust off of them (such occurrences are referred to by NASA as "cleaning events"). This happened during the Mars Exploration Rover Opportunity's mission [13]. The left image in Figure 11 shows a thick layer of accumulated dust on Opportunity in January 2014. The right image shows the solar panels on the rover after a "cleaning event" in late March 2014, which resulted in a power level increase of 70% when compared to previous power levels that year [13]. Such "cleaning events" actually extended the missions of Spirit and Opportunity years beyond their initial three-month duration expectancies.

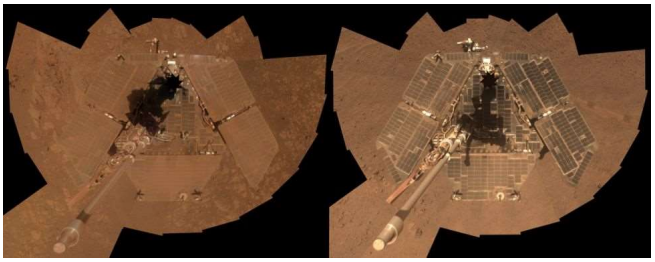

Figure 11. NASA's Mars Exploration Rover, Opportunity, before (left) and after (right) dust was blown off Solar Panels by wind [13]. Images courtesy of NASA/JPL-Caltech/Cornell Univ./Arizona State Univ.

Possible solutions to the dust accumulation problem have been explored by several groups ([6], [8]). To avoid modifying the rovers themselves, NASA has explored alternate mission approaches. In [6], Landis et. al. at NASA detail the exploration of shortening missions to 30-sols (Martian days) as opposed to 90-sols, restricting the rover's daily driving to periods during which more solar power is available, and launching the rover a few months earlier to take advantage of more favorable conditions ("seasons") on Mars. In [8], Mazumder et. al. describe the development of transparent flexible dust shields to minimize obscuration of solar panels (on Mars and Earth) from the accumulation of dust. The dust shields were designed to repel dust particles via an electrostatic charge, enabling solar panels to perform self-cleaning operations. However, they suggest such self-cleaning solar panels equipped with these dust shields could be manufactured to derive their power (for the electrostatic charge) from the solar panels themselves. Depending on the thickness of the accumulated dust, the available power could prove to be insufficient.

Emulation with TREE: Tip and Tendril Coordination

A robot like the TREE could help clean off the solar panels in this scenario. In the movie, *The Martian* [14], Ridley Scott et. al. show Mark Watney (played by Matt Damon) flipping over and blowing off the solar panels that were overturned by the storm that ultimately left him stranded on Mars. If NASA had a robot like the TREE mounted on the Mars rover, astronauts or engineers could routinely clean the solar panels (potentially remotely).

To simulate this type of environment, using a small solar panel covered in red clay particles, we created an environment as shown in Figure 12. As shown in image (a) in the top left corner of Figure 12, the experiment begins with the solar panel covered by a significant layer of "Mars dust" (red clay). The distal section of TREE moves up and down slowly while air blows through it to remove the dust from the solar panel. Then it rotates clockwise 90 degrees as in Figure

12 (b) to enable it to move left and right as it blows more dust away. After a few full sweeping motions, the left (now top) Tendril branch, through which the inspection camera is deployed, extends and bends downward towards the solar panel (Figure 12 (c)). This allows the operator of the TREE to see how much dust the distal section left behind. The viewpoints from the Tendril branch camera are shown in Figure 13 and correspond in sequence to the letters in Figure 12. Finally, the right (now bottom) Tendril branch extends and uses the small brush attached to its tip to sweep away the remaining dust particles from the solar panel, as shown in Figures 12 (d) and 14. This process can be automated or controlled by the TREE's operator.

This solar panel cleaning experiment utilized all degrees of freedom of the distal section of the TREE trunk, as well as the two Tendril branches. This demonstrates the versatility of the robot.

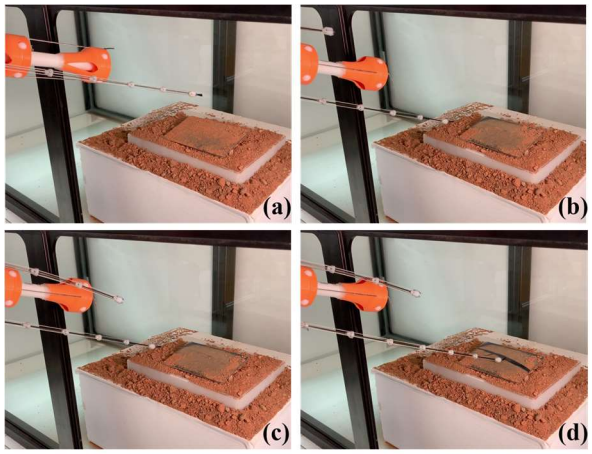

Figure 12. Simulated Mars solar panel dust removal experiment

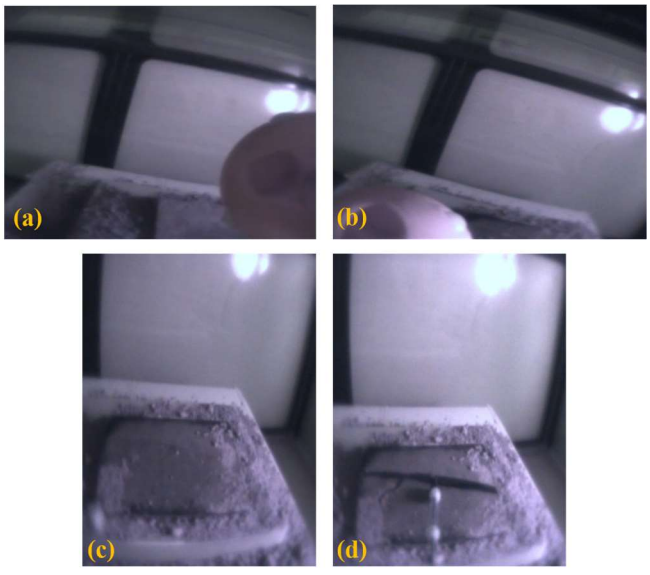

Figure 13. Tendril branch camera view of simulated Mars solar panel dust removal experiment

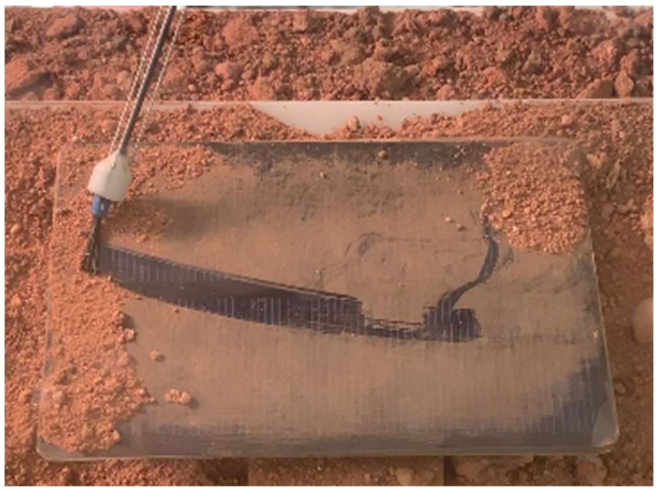

Figure 14. Clean sweep performed by Tendril branch during the dust removal experiment

Tendril-Specific Cleaning

A second experiment, showcasing the capabilities of the Tendril pair in cleaning the remaining dust particles after the blowing of air is reported next. In this experiment, only the branches of the TREE are used to fine clean the solar panel. A brush made from part of a microfiber dust sweeper was attached to the tip of one Tendril branch. The experiment again begins with the solar panel covered by a layer of "Mars dust" (red clay), as shown in Figure 15 (a). The branch extends out to its full length to reach the surface of the solar panel. This extension cleans off a vertical portion of the panel as see in Figure 15 (b). After reaching its maximum length, the branch sweeps orthogonally to the right to continue its cleaning (Figure 15 (c)) and then back to its initial position in the middle (Figure 15 (d)). The other Tendril branch is again used as an inspection camera so that the operator can see the performance of the TREE branch cleaning. The view from the Tendril branch camera is shown in Figure 16. This position of the branch seen in Figure 16 corresponds with the position of the branch in Figure 15 (c). The fine cleaning process with the Tendril branch can be automated or controlled by the TREE's operator.

This experiment utilized the two Tendril branches of the TREE robot. This demonstrates the full planar range of cleaning motion of the branches and their capability to perform fine cleaning operations.

Note that while a similar solar panel cleaning functionality could be provided by a conventional manipulator, augmented with an air tube for blowing, the continuum nature of the TREE allows it to be deployed through tight spaces, which is convenient for both stowage and transport. An additional advantage is that the trunk is hollow, allowing easy deployment of the hose for the blowing operation, as well as for routing sensor (e.g. tip camera) cables. Continuum robot structures are also inherently lightweight, which is an advantage for space-deployed hardware that needs to be cost-effective to launch.

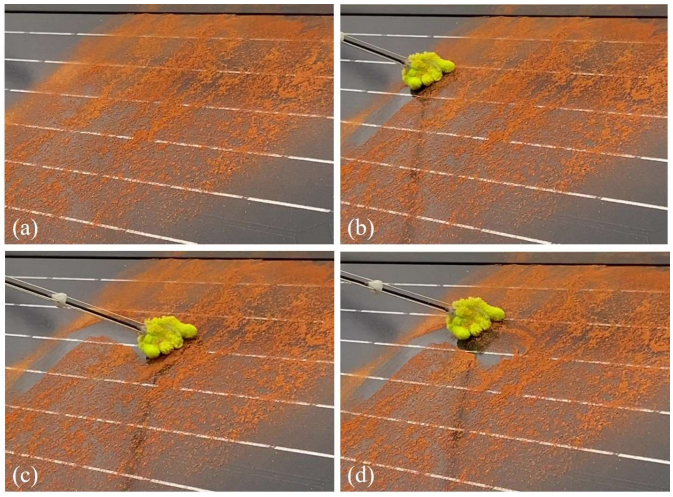

Figure 15. Simulated Mars solar panel fine cleaning experiment

Figure 16. Tendril branch camera view of simulated Mars solar panel fine cleaning experiment

Other Potential Applications

Another field in which the features of blowing and inspecting could be useful is underwater archeology. Scientists use remotely operated vehicles (ROVs) to explore the ocean floor at depths that exceed safe levels for human divers. A system like the TREE integrated into an ROV could assist scientists in gently uncovering buried debris (or potentially treasure) from shipwrecks. At the time of writing, we are using the TREE to conduct further experiments to empirically emulate these applications.

There are also numerous potential medical applications for variable topology robots. The ability to enter the body through a narrow entry port, and to expand to deploy sensors and tools in voids within the body with compliant structures, is at the heart of minimally invasive surgery. While medical applications have not been the aim of our research, which is explicitly focused on larger scale implementations of the concentric tube design [7], there are ongoing efforts in this area, as described in [1].

5. SUMMARY

We have discussed the potential of continuum robots with variable topology for innovative inspection and manipulation operations. Specifically, we have explored a "tree-like" variable topology design, featuring a compliant continuous backbone "trunk" and two pairs of fully retractable continuum appendages: "tendrils" for inspection and cleaning and "roots" for physically stabilizing the system. Via a prototype of the design, we demonstrate the potential for innovative and effective tasks, focusing on the robotic cleaning of solar panels.

ACKNOWLEDGEMENTS

This work was supported in part by NASA under contract NNX12AM01G, and in part by the U.S. National Science Foundation under grants IIS-1527165 and IIS-1718075.

REFERENCES

[1] R. Buckingham, "Snake Arm Robots," Industrial Robot: An International Journal, vol. 29, no. 3, 2002, pp. 242-245.

[2] J. Burgner-Kahrs, D.C. Rucker, H. Choset, "Continuum Robots for Medical Applications," in IEEE Transactions on Robotics, vol. 31, no. 6, December 2015, pp. 1261-1280.

[3] E. Coleshill, L. Oshinowo, R. Rembala, B. Bina, D. Rey, and S. Sindelar, "Dextre: Improving Maintenance Operations on the International Space Station", Acta Astronautica, Volume 64, Issues 9-10, May-June 2009, pp. 869-874.

[4] S. Hirose, Biologically Inspired Robots: Oxford University Press, 1993.

[5] B. A. Jones and I. D. Walker, "Kinematics for multisection continuum robots," IEEE Transactions on Robotics, vol. 22, no. 1, pp. 43-55, Feb 2006.

[6] G.A. Landis, T.W. Kerslake, P. Jenkins, and D. Scheiman, "Mars solar power," in 2nd International Energy Conversion Engineering Conference (IECEC). Providence, Rhode Island: American Institute of Aeronautics and Astronautics, August 2004.

[7] M.C. Lastinger, S. Verma, A.D. Kapadia, and I.D. Walker, "TREE: A Variable Topology, Branching Continuum Robot", Proc. IEEE International Conference on Robotics and Automation, Montreal, Canada, May 2019, pp. 5365-5371.

[8] M. Mazumder, R. Sharma, A. Biris, J. Zhang, C. Calle, and M. Zahn, "Self-cleaning transparent dust shields for protecting solar panels and other devices," Particulate Science and Technology, vol. 25, no. 1, pp. 5-20, 2007. [Online]. Available: https://doi.org/10.1080/02726350601146341

[9] J.S. Mehling, M.A. Diftler, M. Chu, and M. Valvo, "A Minimally Invasive Tendril Robot for In-Space Inspection", Proceedings BioRobotics 2006 Conference, pp. 690-695.

[10] D. Nahar, P.M. Yanik, and I.D. Walker, "Robot Tendrils: Long, Thin Continuum Robots for Inspection in Space Operations", Proc. IEEE Aerospace Conference, Big Sky, MT, March 2017, pp. 1-8.

[11] NASA/JPL-Caltech/Cornell University. (2006, January) "PIA03272: Still shining after all this time (vertical)." [Online]. Available: https://photojournal.jpl.nasa.gov/catalog/PIA03272

[12] NASA/JPL-Caltech/Cornell University. (2007, December) "Mars rover investigates signs of steamy Martian past: Dusty solar panels on spirit." [Online]. Available: https://mars.jpl.nasa.gov/mer/gallery/press/spirit/20071210a.html

[13] I. O'Neill. (2014, April) "Opportunity: The amazing self-cleaning mars rover (photos)." [Online]. Available: https://www.space.com/25577-mars-rover-opportunity-solar-panels-clean.html

[14] R. Scott, "The Martian," 20th Century Fox, 2015, Motion Picture directed by Ridley Scott, screenplay by Drew Goddard, based on the novel by Andy Weir. Starring Matt Damon. (US/UK).

[15] M.M. Tonapi, I.S. Godage, and I.D. Walker, "Next Generation Rope-Like Robot for In-Space Inspection", Proc. IEEE Aerospace Conference, Big Sky, MT, March 2014, pp. 1-12.

[16] D. Trivedi, C.D. Rahn, W.M. Kier, I.D. Walker, "Soft Robotics: Biological inspiration, state of the art, and future research", in Applied Bionics and Biomechanics, Vol. 5, No. 3, September 2008, pp. 99-11.

[17] I.D. Walker, "Continuous backbone "continuum" robot manipulators: A review," ISRN Robotics, vol. 2013, no. 1, pp. 1-19, Jul. 2013.

[18] I.D. Walker, "Robot Strings: Long, Thin Continuum Robots", Proc. IEEE Aerospace Conference, Big Sky, MT, March 2013, pp 1-12.

[19] R. J. Webster Ill and B. A. Jones, "Design and kinematic modeling of constant curvature continuum Robots: A review," International Journal of Robotics Research, Vol.29, No. 13, June 2010, pp. 1661-1683.

[20] M.B. Wooten and I.D. Walker, "A Novel Vine-Like Robot for In-Orbit Inspection", Proc. 45th International Conference on Environmental Systems, Bellevue, WA, July 2015, pp. 1-11.

[21] M.B. Wooten, C.G. Frazelle, I.D. Walker, A.D. Kapadia, and J.H. Lee, "Exploration and Inspection with Vine-Inspired Continuum Robots", Proc. IEEE International Conference on Robotics and Automation (ICRA), Brisbane, Australia, May 2018, pp. 5526-5533.

BIOGRAPHY

Michael C. Lastinger *received a B.S. in Computer Systems Engineering from the University of Georgia in 2016. He conducted the research presented in this paper while pursuing his M.S. in Computer Engineering at Clemson University, which he earned in 2019. He currently works as a Computer Engineer for a private defense and aerospace contractor in Huntsville, AL.*

Allyanna Rice *is an undergraduate student at Clemson University studying Electrical Engineering. She conducted the research presented in this paper while participating in undergraduate honors research. She plans to graduate from Clemson in May of 2020 and pursue a graduate degree.*

Apoorva Kapadia *received a B.E. in Instrumentation Engineering from Mumbai University, India in 2002. He further earned M.S and Ph.D. degrees in Electrical Engineering from Clemson University in 2004 and 2013 respectively. He is currently a Visiting Assistant Professor in the Electrical & Computer Engineering department at Clemson University and spends his spare time looking into continuum robot design and application paradigms along with novel uses of embedded systems.*

Ian D. Walker *received the B.Sc. Degree in Mathematics from the University of Hull, England, in 1983 and the M.S. and Ph.D. Degrees in Electrical and Computer Engineering from the University of Texas at Austin in 1985 and 1989, respectively. He is currently a Professor in the Department of Electrical and Computer Engineering at Clemson University. Professor Walker's research centers on robotics, particularly novel manipulators and manipulation. His group conducts basic research in the construction, modeling, and application of biologically inspired "trunk, tentacle, and worm" robots.*